then acquired of each tube. The procedure was repeated with the 10 mM ME^{ox} solution being replaced by the 10 mM SDS solution.

The peaks in the NMR spectrum corresponding to oxidized and reduced mercaptoethanol were integrated. The changes in these integrals over time were used to calculate the rate of reduction $[(1/c_{final} - 1/c_{initial}) = kt]$ ($k = 0.0044$ mM^{-1} min^{-1}). A similar procedure was used for

sucrose disulfide ($k = 0.0067$ mM^{-1} min^{-1}).

Electrochemical and Electronic Properties of Neutral and Oxidized Soluble Orthogonally-Fused Thiophene Oligomers

**J. Guay,[†] A. Diaz,*,[†] Ruilian Wu,[‡] and James M. Tour*,[‡]**

Contribution from the IBM Research Division, Almaden Research Center, 650 Harry Road, San Jose, California 95120, and the Department of Chemistry and Biochemistry, University of South Carolina, Columbia, South Carolina 29208. Received July 23, 1992

Abstract: The chemical and electrooxidation of spiro-fused thiophene trimers, SIII, and spiro-fused thiophene heptamers, SVII, with terminal α-Si(CH$_3$)$_3$ and β-CH$_3$ groups were studied in CH$_2$Cl$_2$ at room temperature. The heptamer segments in SVII oxidize stepwise to produce the mono radical cation, the bis(radical cation), the radical cation/dication, and the bis(dication), respectively. The existence of these intermediate ions was confirmed by vis/near-IR and ESR analyses. The presence of anodic peaks at different potentials for the removal of the first and second electron from SIII and SVII suggests that some interaction exists between the radical cation and the neutral oligomers. However, once both oligomers are oxidized, there appears to be no significant electronic interactions between the orthogonally positioned heptamer cations except possibly some weak magnetic coupling. With SIII, the trimer segments oxidize at fairly anodic potentials, and the four sequential intermediates are not observed because the less stable cations probably dimerize to form a bis(spiro structure) containing a thiophene hexamer cation.

Introduction

Aviram recently suggested that molecules which are 50 Å long and which contain units that can be independently switched in an electric field would be suitable for interconnections in molecular electronic devices for memory, logic, and amplification.[1] Electronically conducting polymers such as polypyrrole,[2] polyaniline,[3] and polythiophene[4] are, in principle, good candidates for applications in this nanotechnology[7,8] because they have adjustable electrical, optical, and chemical properties.[5,6] The corresponding oligomers have also been considered,[1] and, in particular, thiophene oligomers which are orthogonally-fused at 90° via a saturated spiro-σ structure were proposed to possess the desired switching properties for these applications. A novel route to Aviram's hypothetical structure and other model molecules was recently developed.[9,10] In these structures, the oligomers possess alkyl groups to improve their solubility and terminal trimethylsilyl (α-TMS) groups which permit a further chemoselective modification of the orthogonally-fused oligomers as desired.[10] For these applications, the interactions between the two π-systems must be small so that an oxidized and a neutral oligomer can coexist in the absence of an external bias and not exchange electrons. In

Chart I
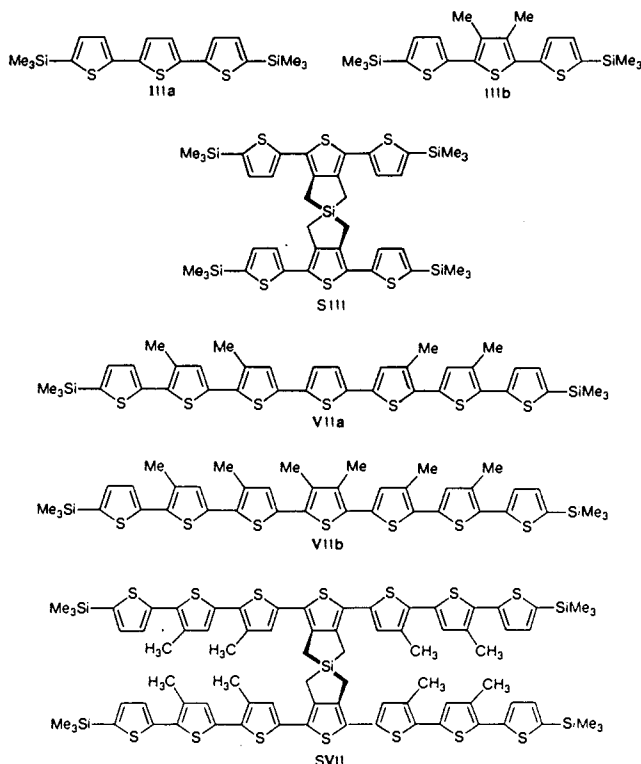
the spiro-fused structure, the oxidized (conducting) and the neutral (nonconducting) states can serve as a bit in a binary system where one state is "one" and the other state is "zero".[1]

In this paper we report the electrochemical and chemical oxidation behavior of spiro-fused thiophene trimers and heptamers and use the corresponding singular thiophene oligomers as ref-

(1) Aviram, A. *J. Am. Chem. Soc.* **1988**, *110* 5687.
(2) Diaz, A. F.; Kanazawa, K. K.; Gardini, J. P. *J. Chem. Soc., Chem. Commun.* **1979**, 635.
(3) Diaz, A. F.; Logan, J. A. *J. Electroanal. Chem.* **1980**, *111*, 111.
(4) Diaz, A. F. *Chem. Scr.* **1981**, *17*, 142.
(5) Skotheim, T. A., Ed. *Handbook of Conducting Polymers*; Marcel Dekker: New York, 1986; Vols. 1 and 2.
(6) Ofer, D.; Crooks, R. M. Wrighton, M. S. *J. Am. Chem. Soc.* **1990**, *112*, 7869.
(7) Franks, A. *J. Phys. E: Sci. Instrum.* **1987**, 1442.
(8) Carter, F. L., Ed. *Molecular Electronic Devices*; Marcel Dekker: New York, 1982 (Vol. 1) and 1987 (Vol. II).
(9) Tour, J. M.; Wu, R.; Schumm, J. S. *J. Am. Chem. Soc.* **1990**, *112*, 5662.
(10) Tour, J. M.; Wu, R.; Schumm, J. S. *J. Am. Chem. Soc.* **1991**, *113*, 7064.
(11) Guay, J.; Kasai, P.; Diaz, A. F.; Wu, R.; Tour, J. M.; Dao, L. H. *Chem. Mater.*, in press.

Table I. Summary of Electrochemical Data

compd	E_{pa1}, E_{pa2}, V (vs SCE)	ΔE_p, mV	$10^5 D$, cm^2/s	n_i, n_t	$h\nu_{max}$, eV
ferrocene	0.64	70	2.55	0.99	
IIIa	1.21, 1.57				3.37
IIIb	1.16, 1.58	90	1.9	0.95	3.56
SIII	1.17, 1.53	150			3.23
VIIa	0.89, 1.07	70, 90	1.2	1.06, 2.1	2.78
VIIb	0.87, 1.05	90, 190			2.92
SVII	0.78, ...^{a}	70	0.9	1.01, 3.9	2.74

^{a} Broad unresolved wave.

erence compounds. We find that the 90° linked thiophene oligomer units can be oxidized both independently and stepwise as in the singular oligomers. With the spiro-fused heptamer, four stable oxidized forms can be generated. The stable oxidized species were also characterized by vis/near-IR and ESR. The results show that the oxidized fused oligomers and the corresponding oxidized singular thiophene oligomers have the same radical cation and dication structures. Furthermore, the spiro-fused thiophene oligomers have little or no intramolecular electronic interactions, while ESR results suggest magnetic interactions.

Experimental Section

The soluble α,α-coupled thiophene oligomers with the terminal α-TMS and β-methyl groups were prepared by Ni- and Pd-catalyzed coupling reactions of the corresponding halide, stannane, or Grignard derivatives as previously described.[12] The preparations of the spiro-fused thiophene trimer and heptamer were also obtained via Pd-catalyzed coupling reactions.[9,10]

The cyclic voltammetry and chronocoulometry experiments were performed with a potentiostat/galvanostat EG&G Model 273 and recorded on an X-Y IBM recorder. The working, counter, and reference electrodes were a 0.5-cm Pt disk, a gold wire, and a SCE double junction containing the electrolyte. Solutions containing 10^{-4} M to 10^{-5} M of the oligomers and 0.1 M Bu$_4$NBF$_4$/CH$_2$Cl$_2$ were used in all electrochemical experiments, and no iR compensation was applied to the cell. Oxidation peak potentials were determined from voltammograms recorded at a 50-mV/s scanning rate, while 10 to 100 mV/s were used to determine the current peak dependence on the sweep rate. Chronocoulometry measurements were made by stepping the potential to 20 mV past the peak potentials and recording the integrated current response with time. The initial potential value was 0.7 for the trimers and 0.5 V for the heptamers. N values were then calculated using the slopes of the i_{pa} versus $\nu^{1/2}$ plot from cyclic voltammetry (Randles–Sevick equation) and of the q versus $t^{1/2}$ plot from the chronocoulometry (Cottrel equation).

Chemical oxidation of the thiophene oligomers was performed according to a procedure similar to that of Fichou et al.[13–15] Solutions of oligomers (20 μM for III and VII and 10 μM for SIII and SVII) and anhydrous FeCl$_3$ (80 μM) were prepared in HPLC grade dichloromethane. For the vis/near-IR and ESR measurements, 80 μM FeCl$_3$ solution was added stepwise to the oligomer solution in a quartz cell or a capillary tube. The final volume was made constant by adding the appropriate amount of dichloromethane, and the spectra were recorded immediately. The oxidation reaction occurs spontaneously as indicated by the rapid color change of the solution which ranges from pink to dark blue depending on the oligomer and the amount of FeCl$_3$ added. The oxidation potential of FeCl$_3$ in dichloromethane is estimated to be 1.22 V (versus SCE) using the Nernst's equation, $E = E^0 + (0.059/n)$ log (C_{ox}/C_{red}), where the formal potential, E^0, was experimentally evaluated to 1.1 V (versus SCE) from the cyclic voltammogram of FeCl$_3$ in dichloromethane. The concentration ratio (C_{ox}/C_{red}) was obtained from the labeled purity of the reagent grade FeCl$_3$ which gives a FeCl$_3$/FeCl$_2$ ratio of 100. The oxidized forms of IIIb, VIIa, VIIb, and SVII in solution were stable enough to record their spectra between 400 and 2000 nm (30 min for each spectrum). Oxidized IIIa and SIII were less stable, and a faster spectrophotometer was used to record their spectra between 200 and 800 nm (1 s of each spectrum).

ESR measurements were performed with a X-band spectrometer ER100D (IBM instruments) at room temperature, at a frequency of 9.76 MHz, with a 1-10-G modulation amplitude and the magnetic field
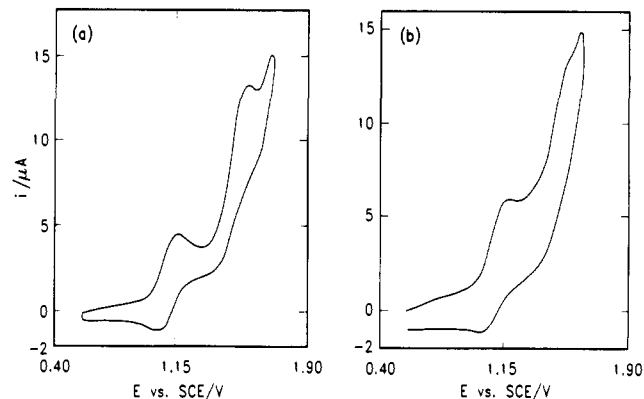
(12) Tour, J. M.; Wu, R. *Macromolecules* **1992**, *25*, 1901.
(13) Fichou, D.; Xu, B.; Horowitz, G.; Garnier, F., *Synth. Met.* **1991**, *41*, 463.
(14) Fichou, D.; Horowitz, G.; Xu, B.; Garnier, F., *Synth. Met.* **1990**, *39*, 243.
(15) Fichou, D.; Horowitz, G.; Garnier, F., *Synth. Met.* **1990**, *39*, 125.

Figure 1. Cyclic voltammogram of (a) IIIb (100 μM) and (b) SIII (100 μM), using a Pt electrode in 0.1 M Bu$_4$NBF$_4$/CH$_2$Cl$_2$ (ν = 50 mV/s).
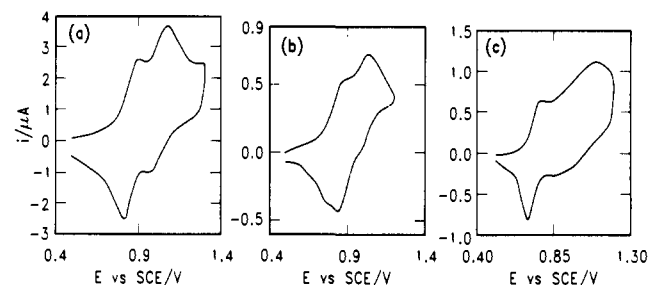

Figure 2. Cyclic voltammogram of (a) VIIa (80 μM), (b) VIIb (8 μM); and (c) SVII (10 μM), using a Pt electrode in 0.1 M Bu$_4$NBF$_4$/CH$_2$Cl$_2$ (ν = 50 mV/s). In (b) and (c) there is a background current correction.

centered at 3.3 kG. Electronic spectra were obtained with a Perkin-Elmer UV/vis/near-IR Lambda 9 spectrophotometer, at room temperature. All spectra are corrected for the solvent absorption.

Results

Electrochemistry and UV–Vis Spectroscopy of the Neutral Oligomers. The cyclic voltammograms of the substituted thiophene oligomers, III and VII, and the spiro-fused oligomers, SIII and SVII, were measured in 0.1 M Bu$_4$NBF$_4$/CH$_2$Cl$_2$ solutions with a scanning rate of 50 mV/s. The voltammograms for the trimer IIIa and IIIb and the spiro-fused SIII show two oxidation processes and only one reduction process on the cathodic sweep. The voltammogram for SIII is shown in Figure 1. The voltammograms for IIIa (not shown) and IIIb are very similar, except that the peaks are superimposed on a large background current. From the size of the reduction peaks, IIIb appears to have a greater chemical reversibility than IIIa. An additional ill-resolved oxidation wave at ca. 1.3 V is seen with SIII. The E_p values are listed in Table I. The data for ferrocene are included for a reference.

The heptamers oxidize at less anodic potentials which reduce the effect of the background current. The voltammograms for the 80-μM VIIa show two well-defined oxidation and reduction waves (Figure 2a), while for 80-μM VIIb, the second oxidation wave is broad and one sharp symmetrical reduction peak appears at 0.8 V in the cathodic sweep. This sharp reduction peak appears with both a gold or a graphite electrode and is not present when the anodic scan is turned around at 0.9 V (before the next peak). With a more dilute solution of VIIb, 8 μM, there is a dramatic decrease in the relative intensity of the sharp reduction peak, and

Orthogonally-Fused Thiophene Oligomers

J. Am. Chem. Soc., Vol. 115, No. 5, 1993 1871

Table II. Summary of $h\nu_{max}$, eV/(λ_{max}, nm) Data

| oligomer	radical cation				dication	
	1	2	3	4	1	2
IIIa			2.16 (574)	2.37 (522)		
IIIb	1.41 (879)	1.59 (781)	2.24 (554)	2.42 (516)		
SIII			2.24 (554)	2.43 (510)		
VIIa	0.69 (1785)	0.87 (1427)	1.49 (834)	1.66 (740)	1.01 (1231)	1.16 (1068)
VIIb	0.73 (1688)	0.89 (1396)	1.55 (800)	1.71 (724)	0.99 (1256)	1.14 (1088)
SVII	0.74 (1672)	0.90 (1390)	1.55 (798)	1.70 (728)	1.01 (1230)	1.16 (1072)

now three reduction peaks are visible (Figure 2b, corrected for background current). Thus the sharp reduction peak must be associated with the weak adsorption of some product from the second oxidation.[16] The cyclic voltammogram of 10 μM SVII (corrected for the background current) also shows several oxidation processes including a broad second wave (300 mV width) involving several oxidation reactions (Figure 2c). The voltammogram of SVII is similar on gold and graphite electrodes, but, in contrast with VIIb, it does not change when the concentration of SVII is varied. In every case, the oxidation current peak values, i_{pa}, scale linearly with the square root of the sweep rate, $\nu^{1/2}$, for ν between 25 and 250 mV/s, which is consistent with a diffusion limited reaction.

It was previously shown with the thiophene oligomers that the α-TMS and β-CH$_3$ groups improve their solubility and stabilize the radical cation.[11] Accordingly, the β-CH$_3$ groups and the spiro bridge cause a cathodic shift of the first oxidation waves. The first oxidation reaction of IIIb which has β-CH$_3$ groups is chemically reversible; it is not with IIIa. The more reactive IIIa radical cation apparently dimerizes since the vis/near-IR absorption bands of the resulting ion closely resemble those for the oxidized hexamer.[11] Oxidation of SIII also leads to some dimerization as evident by the vis/near-IR spectrum (see below). The oxidation of VIIa, VIIb, and SVII is chemically reversible, and the first oxidation reaction of VIIa has ΔE_p equal to 70 ± 10 mV for ν between 25 and 250 mV/s, plus i_{pc}/i_{pa} is ca. unity.

Chronocoulometry experiments were performed only on IIIb, VIIa, and SVII, because they produce relatively stable cations. The number of electrons for the first peak (n_1) and for all the oxidation processes (n_t) and the diffusion coefficients (D) are listed in Table I. The first oxidation peak for IIIb (Figure 1a) corresponds to a one-electron process ($n = 0.95$), and we assume that the first oxidation wave for IIIa and SIII is also a one-electron process because of the similarities between the structures. The two separate oxidations of VIIa both have n equal to 1. With SVII, the first oxidation wave also involves one electron while the second broad anodic wave has n equal to 3. As expected, D is significantly smaller for the larger molecules.

The UV–vis spectra of the oligomers were also recorded in CH$_2$Cl$_2$, and the λ_{max} energies are reported in Table I. The bands correspond to π–π* transitions, and there is only a small difference in the position of the bands between the singular and the spiro-fused oligomers where those for the latter are lower energy. The band intensities for the spiro-fused oligomers are ca. two times greater than for the corresponding singular oligomers (at the same concentration). These results suggest that the orthogonally positioned π-structures in the spiro compounds are fairly independent and free of interactions when neutral. Although III and VII are used as model structures for the thiophene oligomer units in the spiro compounds, structural changes induced by the spiro bridge could affect the π–π* transitions.

Vis/near-IR and ESR of the Oxidized Oligomers. The chemical oxidation of the thiophene oligomers (Th$_n$) with FeCl$_3$[15] allows the stepwise generation of the radical cation (eq 1) and the dication

$$\text{Th}_n + 2\text{FeCl}_3 \rightarrow \text{Th}_n^+ + \text{FeCl}_4^- + \text{FeCl}_2 \qquad (1)$$
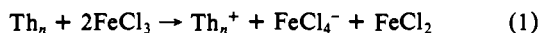
(eq 2). In this study, the oligomers were oxidized in CH$_2$Cl$_2$ by

$$\text{Th}_n^+ + 2\text{FeCl}_3 \rightarrow \text{Th}_n^{2+} + \text{FeCl}_4^- + \text{FeCl}_2 \qquad (2)$$
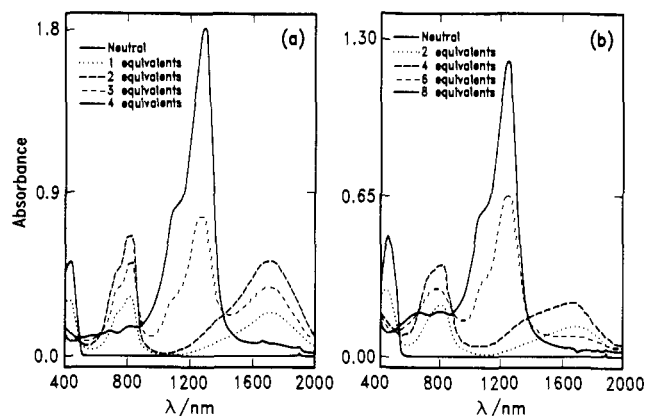

Figure 3. Vis–NIR absorption spectrum of (a) VIIb (10 μM) and (b) SVII (5 μM); spectra in CH$_2$Cl$_2$ after the addition of FeCl$_3$.

adding the appropriate amount of 80 μM FeCl$_3$/CH$_2$Cl$_2$ solution to a measured volume of a 20 μM solution of the oligomer (10 μM for SIII and SVII).

As the radical-cation and dication forms of the oligomers are generated, the π–π* absorption decreases and new transitions emerge in the vis/near-IR region. This is seen in the spectra for the neutral and the oxidized forms of VIIb and SVII in CH$_2$Cl$_2$. The spectra of VIIa are identical with those for VIIb and are not shown. The spectra of IIIb are published[11] and are also omitted here. With IIIb, VIIa, and VIIb, the initial π–π* band intensities are reduced to one-half with the addition of 1 equiv of FeCl$_3$ and completely with 2 equiv. Similar changes occur in the spectra of SIII and SVII when 2 and 4 equiv of FeCl$_3$ are added, but with SIII the π–π* band does not disappear completely even with more than 4 equiv of FeCl$_3$. The radical-cation spectra for VIIb and SVII (and for IIIb and VIIa, not shown) consist of two strong absorptions and shoulder transitions on the high-energy side (Figure 3, a and b). The absorption intensities grow with the addition of 2 and 4 equiv of FeCl$_3$ to the solution of the singular and the spiro-fused oligomers, respectively. IIIa and SIII show a different behavior where the absorption bands that are originally produced by the oxidation gradually decrease in intensity and new bands appear at 689 and 788 nm with IIIa and 702 and 796 nm with SIII. These bands are very close to the λ_{max} values reported for the radical cation of the thiophene hexamer, 693 and 779 nm.[11] This is not surprising since both bithiophene and bithiophene with α-TMS groups dimerize via the α-position when oxidized.[17,18] The dimer that is formed must contain a thiophene trimer, hexamer, and trimer, in that order and each positioned orthogonal to the other. To the extent that the dimer reacts further, it will produce structures which contain orthogonally positioned thiophene hexamers.

The energy and wavelength of the electronic transitions for the thiophene oligomer radical cations are listed in Table II. As expected, the transitions are at lower energies for the larger oligomer. Furthermore, $h\nu_{max}$ values for the SIII and SVII radical cations match those for the IIIb and VIIb radical cations but appear at higher energies than those for IIIa and VIIa. Finally,

(16) Greef, R. et al. In *Instrumental Methods in Electrochemistry*; Kemp, T. J., Ed.; Ellis Horwood: England, 1985 and references therein.

(17) Xu, Z.; Fichou, D.; Horowitz, G.; Garnier, F. *J. Electroanal. Chem.* **1989**, *267*, 339.

(18) Lemaire, M.; Buchner, W.; Garreau, R.; Hoa, H. A.; Guy, A.; Roncali, J. *J. Electroanal. Chem.* **1990**, *281*, 293.

1872 *J. Am. Chem. Soc., Vol. 115, No. 5, 1993*
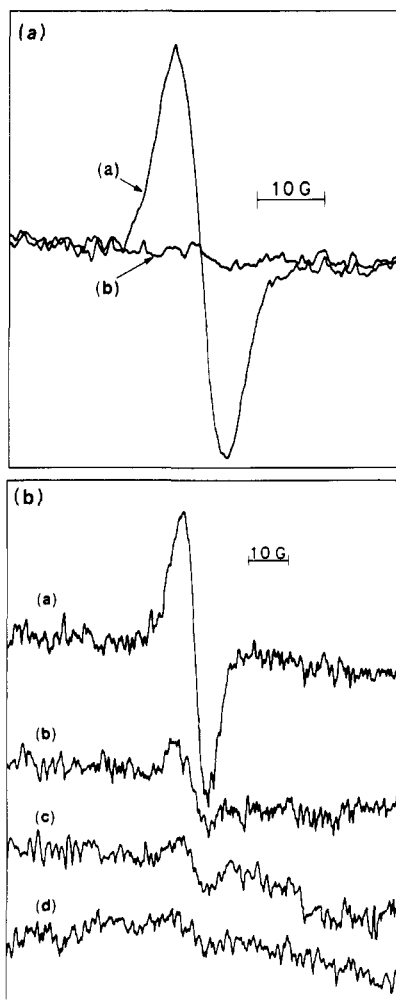
Guay et al.

Figure 4. ESR spectra of chemically oxidized (a) VIIa using (a) 2 and (b) 4 equiv of $FeCl_3$, and (b) SVII using (a) 2, (b) 4, (c) 6, and (d) 8 equiv of $FeCl_3$.

the main peak and the shoulder are separated by ca. 0.17 eV which agrees with our previous observations with the singular oligomers.[11]

The subsequent addition of $FeCl_3$ to the oligomer radical-cation solutions leads to new absorption bands in the vis/near-IR spectra for VIIb (Figure 3a), SVII (Figure 3b), and VIIa (not shown). The band intensities for the radical cations decrease, and two new ill-resolved strong transitions grow in their spectra as $FeCl_3$ is added incrementally. The new peaks, probably dication transitions, increase to a maximum intensity when a total of 4 equiv of $FeCl_3$ is added to VIIa and VIIb and 8 equiv for SVII. At this point, the bands for the radical cations have vanished in line with the stoichiometry in eq 2. The absorption maxima are listed in Table II. In contrast with the radical cations, with the dications the transition energies for SVII and VIIa are now identical while those for VIIb are slightly different. It is also interesting to note that the two transitions for VIIa, VIIb, and SVII dications are separated by 0.15 eV. The origin of the transitions of the oligomer dications was previously discussed.[11] In contrast, IIIb radical cation is not oxidized further by $FeCl_3$ owing to its limited oxidation capacity in CH_2Cl_2 of ca. 1.22 V.[11]

The oligomer solutions used for the ESR spectroscopy analysis were prepared as for the vis/near-IR (vide infra) analysis. Figure 4a shows the ESR spectra of VIIa after the addition of 2 (a) and 4 (b) equiv of $FeCl_3$. The spectra for VIIb are almost identical with those for IIIb which were previously reported.[11] With the addition of 2 equiv of $FeCl_3$, each oligomer displays a strong and narrow ESR signal centered at $g = 2.004$ with $\Delta H_{pp} = 8$ G as is typical for organic radicals. The signal intensity grows with added $FeCl_3$ to a maximum intensity with 2 equiv. At this point, the signal intensity corresponds to the quantitative conversion of

the neutral spiro-fused oligomers to the mono radical cations. Figure 4b shows the ESR spectra of SVII after the addition of 2 (a), 4 (b), 6 (c), and 8 (d) equiv of $FeCl_3$. Again, the maximum signal, $\Delta H_{pp} = 8$ G, is also obtained with 2 equiv of $FeCl_3$. As expected, the relative signal intensity for VIIa (20 μM) is ca. twice that for SVII (10 μM) after 2 equiv of $FeCl_3$ was added (removal of one electron per molecule). Thus, the neutral oligomers are oxidized to the radical cation following the stoichiometry in eq 1.

The ESR signal of VIIa and SVII vanishes almost completely with the subsequent addition of 4 and 8 equiv of $FeCl_3$, respectively, owing to the generation of the diamagnetic species as in eq 2. At the high $FeCl_3$ concentrations, only a residual signal due to the paramagnetic $FeCl_4^-$ ions in solution is observed. This signal is much weaker and broader, $\Delta H_{pp} = 400-600$ G, and is centered at $g = 2$. VIIb had the same behavior as VIIa. With IIIb the ESR signal remains unchanged.

Discussion

It was previously shown that thiophene oligomers undergo two stepwise one-electron oxidations to produce the radical cation and dication, respectively.[11] The cyclic voltammogram of SVII reveals that it is oxidized in voltage range 0.6 to 1.2 V. The first oxidation ($n = 1$) is a single wave, and the subsequent oxidations (three electrons) are included in the broad rather featureless wave between 0.8 and 1.2 V. The foot of the second oxidation wave for SVII (Figure 2b) shows a hump at ca. 0.9 V, which may be the second one-electron oxidation reaction. The poor peak resolution is not surprising considering their proximity (<100 mV).[19] The peak separations, however, are small compared with the ca. 500-mV separations observed with the oligomeric silicon phthalocyanines and the dichromium complexes which are known to possess significant electron interactions.[20,21] The more anodic voltage required to remove the second electron from SVII suggests that there is some interaction between the neutral and the radical-cation forms in the molecule, although a peak separation of ca. 40 mV is expected for molecules having negligible interactions between the electroactive centers.[19]

The total of four electrons involved in the complete electro-oxidation of SVII agrees with the 8 equiv of $FeCl_3$ used in the chemical oxidation. The stepwise oxidation of the oligomers to generate the various cations shown in Scheme I is best accomplished with $FeCl_3$. The vis/near-IR spectra indicate that, with 4 equiv of $FeCl_3$ (2 equiv per oligomer unit), only radical cations are generated, i.e., the SVII bis(radical cation). This conclusion is supported by the comparison of the radical-cation spectra of SVII which was obtained using 2 and 4 equiv of $FeCl_3$ (Figure 3b) with the spectra of VIIa and VIIb (Figure 3a). The signal intensity for SVII increases with added $FeCl_3$ up to 2 equiv, consistent with the formation of the radical cations.

With additional amounts of $FeCl_3$ beyond 2 equiv of $FeCl_3$, the signal surprisingly decreases, and with 4 equiv it is only 10% of the expected intensity for two radical cations even though the vis/near-IR spectra indicate the bis(radical cation) is being generated. The abnormally low signals indicate some form of interaction, possibly some internal through-space magnetic coupling (triplet radical pair) between the two orthogonally positioned radical cations in the SVII bis(radical cation). This coupling is known to decrease the ESR signal of an unpaired radical to produce a pattern with splitting factors as high as 350 G.[22] In our case, this signal would be masked by the paramagnetic signal of $FeCl_4^-$. Intermolecular magnetic coupling may also be present and be more important for the SVII radical cation/dication which also shows a low signal and where internal magnetic coupling is not possible. Disproportionations to produce the neutral and the
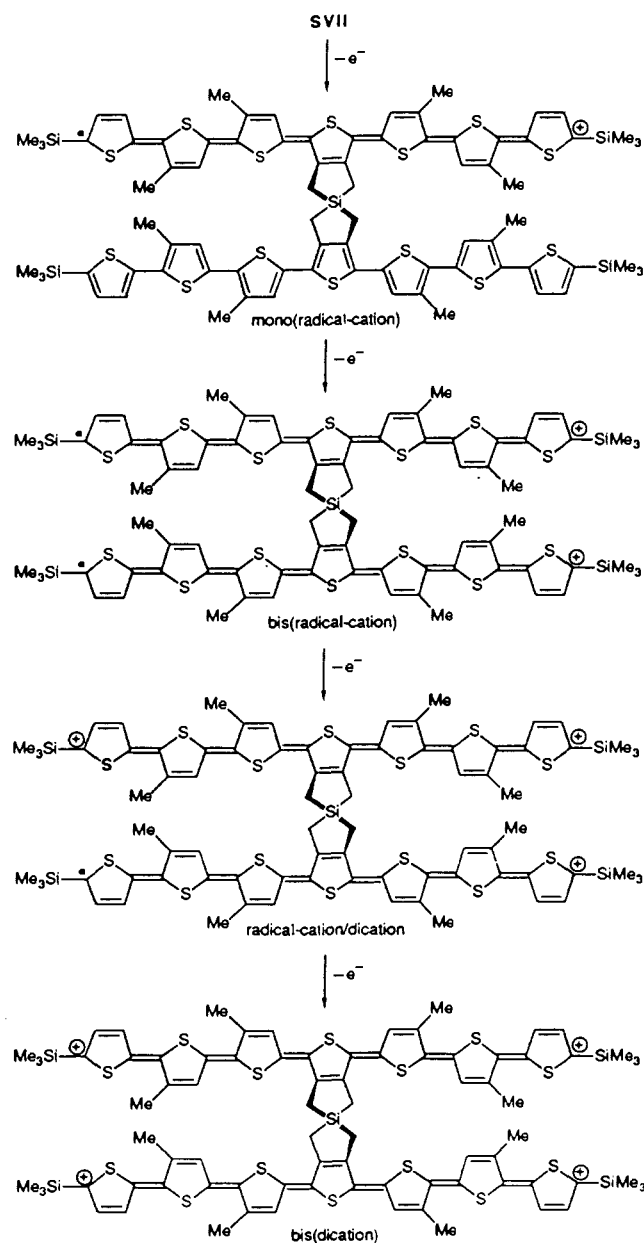
(19) Ammar, F.; Saveant, J. M. *J. Electroanal. Chem.* **1973**, *47*, 215.
(20) DeWulf, D. W.; Leland, J. K.; Wheeler, B. L.; Bard, A. J.; Batzel, D. A.; Dininny, D. R.; Kenney, M. E. *Inorg. Chem.* **1987**, *26*, 266.
(21) Van Order N., Jr.; Geiger, W. E.; Bitterwolf, T. E.; Rheingold, A. L. *J. Am. Chem. Soc.* **1987**, *109*, 5680.
(22) Hatton, W. G.; Hacker, N. P.; Kasai, P. H. *J. Chem. Soc., Chem. Commun.* **1990**, 227.

Scheme I

SVII

|−e⁻

Me₃Si ... [thiophene oligomer structure] (+) SiMe₃

Me₃Si [thiophene oligomer structure] SiMe₃

mono(radical-cation)

|−e⁻

Me₃Si ... [thiophene oligomer structure] (+) SiMe₃

Me₃Si ... [thiophene oligomer structure] (+) SiMe₃

bis(radical-cation)

|−e⁻

Me₃Si (+) [thiophene oligomer structure] (+) SiMe₃

Me₃Si ... [thiophene oligomer structure] (+) SiMe₃

radical-cation/dication

|−e⁻

Me₃Si (+) [thiophene oligomer structure] (+) SiMe₃

Me₃Si (+) [thiophene oligomer structure] (+) SiMe₃

bis(dication)

dication forms does not occur and would be readily evident in the vis/near-IR spectra.

Accompanying the further oxidation of SVII with 6 and 8 equiv of FeCl₃ is the appearance of two new bands in the vis/near-IR spectra (Figure 3a) and a simultaneous decrease of the band intensity for the radical cation. The new bands are assigned to the dications based on the very close resemblance of spectra to the spectra for the VIIa and VIIb (Figure 3a) dications. Thus, the removal of a third electron leads to a spiro molecule bearing a heptamer radical cation and a heptamer dication (see Scheme I). However, the corresponding ESR signal (Figure 4b (c)) has not changed significantly from the signal for the bis(radical-cation) (Figure 4b (b)). The removal of the fourth electron (8 equiv of FeCl₃) generates the quadruply charged SVII ion with the two dications orthogonally positioned in the spiro molecule. There is now no corresponding ESR signal as is expected for dications (Figure 4b (d)). As previously noted for a series of thiophene oligomers, with 3 to 8 units, the charge in the radical cation and dication is delocalized over the entire π-structure.[11]

The very close resemblance of the vis/near-IR spectra between the spiro-fused SVII and VII (Table II) suggests that there are no significant π-electron through-space or through-bond interactions[23,24] between the orthogonally positioned oligomer units

whether they are completely neutral or in any of the cationic forms. The small differences observed in the vis/near-IR spectra may result from minor geometrical effects on the oligomers in the spiro structure or differences in solvation energies.[25,26] Even if some interactions exist between the units of SVII mono radical cations, there is probably no electron exchange since this would lead to either a broadening of the ESR signal or hyperfine structure for very fast electron exchange.[27] However, since the intensity and ΔH_{pp} of the ESR signal for SVII radical cation are almost identical with those for VIIa and VIIb radical cations, electron exchange must be less than 10^8 s⁻¹, the ESR time scale. This is consistent with the vis/near-IR spectral data since the observation of the electronic transitions for both the neutral and the radical-cation forms imply an electron exchange rate in picoseconds.

The cyclic voltammogram of SIII (Figure 1b) resembles those of IIIa and IIIb (Figure 1a) except for the broad wave between the two main oxidation waves. Since the first oxidation of IIIb involves one-electron transfer and since the chemical oxidation of IIIb and SIII follow the stoichiometry of eq 1, we can assume that the first peak for SIII is also a one-electron oxidation. The middle wave located at 1.3 V may be due to the removal of the second electron from the second thiophene trimer in SIII to produce the bis(radical cation), although it could also result from the oxidation of extraneous material. Again as with SVII, the different potentials for the removal of the first and second electron suggest that there is some interaction between the neutral and the radical-cation forms of the oligomers in the molecule. The third oxidation wave at ca. 1.58 V probably transforms one trimer radical cation into the dication. Unfortunately, the oxidation potential of the FeCl₃ solution is not high enough to further oxidize SVII for spectroscopic analysis.

The rigid σ-structure of these spiro molecules prevents the formation of internal π-dimers of the type proposed to exist with the oxidized 2,5″-dimethylterthiophene (π-stacking) to explain the decrease in the ESR signal and the presence of additional bands in the UV–vis spectra of the oligomer.[28,29] Likewise, no evidence of external π-dimers is seen in the electronic spectra of oxidized SII and SVII, which parallels our previous observations with IIIa, IIIb, VIIa, and VIIb.[11] Furthermore, the ESR signal intensity corresponds to the quantitative conversion of neutral oligomers to the mono radical cations. While π-dimer formation may be less favorable because of the substituents, even the radical cations of the unsubstituted 2,5-linked thiophene pentamer and hexamer[15] do not provide evidence for π-dimer formation at room temperature. Besides the structural effects, π-dimerization has been proposed to explain the results obtained under experimental conditions which are significantly different from those in our and in Fichou's experiments.[16] π-Dimerization has been observed with the electrooxidized trimer monomer radical cations in acetonitrile electrolyte between −30 to +5 °C, and with photooxidized trimers in CH₃CN–CF₃COOH solution.[28,29]

Finally, through-space magnetic coupling as described here may explain the small number of spins found in the oxidized films of polythiophene and other polymers. π-Dimers were proposed to explain the low number of spins in oxidized polythiophene film because their presence increases with the oligomer concentration,[28,29] and the solid-state polythiophene films certainly represent the highly concentrated case. However, these proposals do not explain the ESR results for substituted polythiophene in solution which show an increase in the number of spins as the polymer concentration increases.[29]

(23) Paddon-Row, M. N. *Acc. Chem. Res.* **1982**, *15*, 245 and references therein.

(24) Beratan, D. N.; Onuchic, J. N.; Hopfield, J. J. *J. Chem. Phys.* **1985**, *83*, 5325.

(25) Zuman, P. In *Substituent Effects in Organic Polarography*; Plenum Press: New York, 1967.

(26) Parker, V. D. *J. Am. Chem. Soc.* **1976**, *98*, 98.

(27) Kasai, P. Private communication.

(28) Hill, M. G.; Mann, K. R.; Miller, L. L.; Penneau, J. F. *J. Am. Chem. Soc.* **1992**, *114*, 2728.

(29) Hill, M. G.; Penneau, J. F.; Mann, K. R.; Miller, L. L. *Chem. Mater.* in press.

Conclusions

In conclusion, the spiro-fused thiophene trimer, SIII, and spiro-fused thiophene heptamer, SVII, with terminal α-TMS and β-CH$_3$ groups were readily oxidized in CH$_2$Cl$_2$ both electrochemically and with FeCl$_3$. The thiophene heptamer segments in the spiro-fused SVII can be oxidized sequentially with FeCl$_3$ to produce the mono radical cation, the bis(radical cation), the radical cation/dication, and the bis(dication), respectively. The existence of these intermediate ions was confirmed by vis/near-IR and ESR analyses. It was also concluded that there is some interaction between the neutral and the radical-cation forms in SVII, but there is no significant electronic interaction between the orthogonally positioned heptamer radical cations or the di-

cations except possibly some weak magnetic coupling. With SIII, the trimer segments are oxidized at higher voltages, and the four sequential intermediates are not observed because the less stable cations probably dimerize to form a bis(spiro structure) containing thiophene hexamer cation.

Surface Structures of PbS Microcrystals Modified with 4-Hydroxythiophenol and Their Influences on Photoinduced Charge Transfer

Tsukasa Torimoto,[‡] Hiroyuki Uchida,[‡] Takao Sakata,[†] Hirotaro Mori,[†] and Hiroshi Yoneyama*,[‡]

Contribution from the Department of Applied Chemistry, Faculty of Engineering, Osaka University, Yamada-oka 2-1, Suita, Osaka 565, Japan, and Research Center for Ultra-High Voltage Electron Microscopy, Osaka University, Yamada-oka 2-1, Suita, Osaka 565, Japan. Received August 14, 1992

Abstract: Quantized PbS microcrystals capped with 4-hydroxythiophenol (ArSH) were prepared using two different concentration ratios of [Pb^{2+}]/[S^{2-}] = 1.2 and 3.0 with fixed concentration ratio of [ArSH]/[Pb^{2+}] = 4.0. The size distributions of the prepared PbS particles were determined. Two different surface structure models of fully occupied and partially occupied surface sites of PbS microcrystals with the capped ArSH are assumed, and chemical compositions of these particles are evaluated by taking the experimentally determined particle size distributions into account. By examining the fitness of the chemical analyses data of the PbS particles to the evaluated compositions, it is proposed that the PbS particles prepared [Pb^{2+}]/[S^{2-}] = 3.0 had the capped ArSH in all the surface sites, while PbS particles prepared with [Pb^{2+}]/[S^{2-}] = 1.2 had some surface sites free from the modifier. The proposed surface structures of the two kinds of PbS microcrystals were rationalized by experimentally found differences both in agglomeration tendencies of the particles and in the effect of the addition of Pb^{2+} ions on the rate of photoinduced reduction of methyl viologen on the particles.

Introduction

Quantized semiconductor microcrystals have been intensively studied in recent years.[1-5] Synthetic approaches to obtain monodispersed particles with controlled size have been one of the major research interests, and chemical modification by capping with organic reagents seems to be one of the most effective methods to achieve this. For example, thiol and selenol compounds have been successfully used as the capping reagents to prepare quantized CdS, CdSe, CdSe–ZnS, and CdSe–ZnSe particles[6-16] with narrow size distributions in quantized regime.

Physicochemical properties of these semiconductor microcrystals capped with organic moieties have been studied.[6-26] In particular, the structure of these particles have been characterized by TEM,[7,9,11,14] NMR,[17] X-ray diffraction,[9-11,14,21] XPS,[13,14] Auger spectroscopy,[13] and EXAFS.[24] However, the characterization of the capped surface in atomic scale has not yet been reported except, for example, using EXAFS, where atomic rearrangements of CdS and CdSe surfaces on capping with benzeneselenol were suggested.

In cases of capped semiconductor microcrystals, it seems very important to clarify the effect of the capping agent on various properties of semiconductor microcrystals, especially in relation

to detailed surface structures of capped semiconductors. However, presently we have no information about this. So far well-docu-

(1) Henglein, A. *Top. Curr. Chem.* **1988**, *143*, 113–181.

(2) Henglein, A. *Chem. Rev.* **1989**, *89*, 1861–1873.

(3) Steigerwald, M. L.; Brus, L. E. *Annu. Rev. Mater. Sci.* **1989**, *19*, 471–495.

(4) Steigerwald, M. L.; Brus, L. E. *Acc. Chem. Res.* **1990**, *23*, 183–188.

(5) Wang, Y.; Herron, N. *J. Phys. Chem.* **1991**, *95*, 525–532.

(6) Nosaka, Y.; Yamaguchi, K.; Miyama, H.; Hayashi, H. *Chem. Lett.* **1988**, 605–608.

(7) Steigerwald, M. L.; Alivisatos, A. P.; Gibson, J. M.; Harris, T. D.; Kortan, R.; Muller, A. J.; Thayer, A. M.; Duncan, T. M.; Douglass, D. C.; Brus, L. E. *J. Am. Chem. Soc.* **1988**, *110*, 3046–3050.

(8) Hayes, D.; Mićić, O. I.; Nenadović, M. T. Swayambunathan, V.; Meisel, D. *J. Phys. Chem.* **1989**, *93*, 4603–4608.

(9) Dameron, C. T.; Reese, R. N.; Mehra, R. K.; Kortan, A. R.; Carroll, P. J.; Steigerwald, M. L.; Brus, L. E.; Winge, D. R. *Nature* **1989**, *338*, 596–597.

(10) Herron, N.; Wang, Y.; Eckert, H. *J. Am. Chem. Soc.* **1990**, *112*, 1322–1326.

(11) Kortan, A. R.; Hull, R.; Opila, R. L.; Bawendi, M. G.; Steigerwald, M. L.; Carroll, P. J.; Brus, L. E. *J. Am. Chem. Soc.* **1990**, *112*, 1327–1332.

(12) Swayambunathan, V.; Hayes, D.; Schmidt, K. H.; Liao, Y. X.; Meisel, D. *J. Am. Chem. Soc.* **1990**, *112*, 3831–3837.

(13) Hoener, C. F.; Allan, K. A.; Bard, A. J.; Campion, A.; Fox, M. A.; Mallouk, T. E.; Webber, S. E.; White, J. M. *J. Phys. Chem.* **1992**, *96*, 3812–3817.

(14) Colvin, V. L.; Goldstein, A. N.; Alivisatos, A. P. *J. Am. Chem. Soc.* **1992**, *114*, 5221–5230.

[†] Research Center For Ultra-High Voltage Electron Microscopy.

[‡] Department of Applied Chemistry.